HHS Public Access

Author manuscript

Virology. Author manuscript; available in PMC 2022 July 01.

Published in final edited form as:

Virology. 2021 July ; 559: 30–39. doi:10.1016/j.virol.2021.03.014.

Chimeric Zika viruses containing structural protein genes of insect-specific flaviviruses cannot replicate in vertebrate cells due to entry and post-translational restrictions

Chandra S. Tangudu[1], **Jermilia Charles**[1], **Daniel Nunez-Avellaneda**[1], **Alissa M. Hargett**[1], **Aaron C. Brault**[2], **Bradley J. Blitvich**[1,*]

[1]Department of Veterinary Microbiology and Preventive Medicine, College of Veterinary Medicine, Iowa State University, Ames, Iowa;

[2]Division of Vector-Borne Diseases, Centers for Disease Control and Prevention, Fort Collins, Colorado

Abstract

Long Pine Key virus (LPKV) and Lammi virus are insect-specific flaviviruses that phylogenetically affiliate with dual-host flaviviruses. The goal of this study was to provide insight into the genetic determinants that condition this host range restriction. Chimeras were initially created by replacing select regions of the Zika virus genome, including the premembrane and envelope protein (prM-E) genes, with the corresponding regions of the LPKV genome. Of the four chimeras produced, one (the prM-E swap) yielded virus that replicated in mosquito cells. Another chimeric virus with a mosquito replication-competent phenotype was created by inserting the prM-E genes of Lammi virus into a Zika virus genetic background. Vertebrate cells did not support the replication of either chimeric virus although trace to modest amounts of viral antigen were produced, consistent with suboptimal viral entry. These data suggest that dual-host affiliated insect-specific flaviviruses cannot replicate in vertebrate cells due to entry and post-translational restrictions.

[*]Author for correspondence: Bradley J. Blitvich, PhD, 2116 Veterinary Medicine, Iowa State University, Ames, Iowa, 50011, blitvich@iastate.edu, Telephone: 515-294-9861, Fax: 515-294-8500.

Author Contributions

CST performed the majority of the laboratory work, including all of the viral chimera construction. JC, DNA and AMH performed select laboratory experiments, including some of the RNA extractions, RT-PCRs, Western blots, Sanger sequencing and cell culture experiments. BJB and ACB conceived the idea and acquired the funding that supported the study. BJB prepared the first draft of the manuscript. All other authors reviewed the first draft and provided constructive feedback.

COMPETING INTERESTS

None of declare

Declaration of interests

The authors declare that they have no known competing financial interests or personal relationships that could have appeared to influence the work reported in this paper.

Keywords

flavivirus; insect-specific; chimeric; host range; entry

INTRODUCTION

Most viruses in the genus *Flavivirus*, including all four serotypes of dengue virus (DENV1–4), Japanese encephalitis virus (JEV), West Nile virus (WNV), yellow fever virus (YFV) and Zika virus (ZIKV), are maintained in transmission cycles between hematophagous arthropods and vertebrates and therefore, exhibit a dual-host tropism. Others have insect-restricted or vertebrate-restricted host ranges (Blitvich and Firth, 2015, 2017; Bolling et al., 2015; Elrefaey et al., 2020; Roundy et al., 2017). Insect-specific flaviviruses (ISFs) can be separated into two distinct groups: classical ISFs (cISFs) and dual-host affiliated ISFs (dISFs). Classical ISFs (also known as lineage I ISFs) were the first to be discovered and are phylogenetically distinct from all other known flaviviruses. Viruses in this group include cell fusing agent virus, Culex flavivirus, Kamiti River virus, Niénokoué virus, Palm Creek virus and Parramatta River virus (Crabtree et al., 2003; Hobson-Peters et al., 2013; Hoshino et al., 2007; Junglen et al., 2017; McLean et al., 2015; Stollar and Thomas, 1975). Dual-host affiliated ISFs (also known as lineage II ISFs) phylogenetically affiliate with dual-host mosquito-borne flaviviruses (MBFVs), despite their apparent vertebrate-restricted phenotype. MBFVs belong to the vertebrate-infecting flavivirus (VIF) group, which also includes tick-borne flaviviruses. Examples of dISFs include Binjari virus (BinJV), Long Pine Key virus (LPKV), Ilomantsi virus, Lammi virus (LAMV), Nhumirim virus and Nounané virus (Guzman et al., 2018; Hobson-Peters et al., 2019; Huhtamo et al., 2014; Huhtamo et al., 2009; Junglen et al., 2009; Pauvolid-Correa et al., 2015).

Based on their phylogenetic placement with dual-host MBFVs, it has been hypothesized that dISFs are dual-host viruses with an unidentified vertebrate host or ISFs that recently lost the ability to infect vertebrates (Kenney et al., 2014). The second hypothesis is favored because the replicative abilities of several dISFs have been assessed in numerous vertebrate cell lines with none of the cell lines able to support prolonged virus replication (Huhtamo et al., 2014; Huhtamo et al., 2009; Junglen et al., 2009; Kenney et al., 2014). Analysis of the codon usage preferences of dISFs revealed a bias for mosquito growth, but it is not as extreme as observed for cISFs (Blitvich and Firth, 2015; Colmant et al., 2017). Dual-host affiliated ISFs are not monophyletic; phylogenetic studies have shown that these viruses form two distinct subclades in the dual-host MBFV clade, suggesting that separate evolutionary events were responsible for the loss of vertebrate host replication for each subclade (Blitvich and Firth, 2015). One subclade consists of dISFs isolated primarily from *Aedes* spp. mosquitoes and the other consists of dISFs isolated primarily from *Culex* spp. mosquitoes. LPKV and LAMV are *Aedes*-associated viruses (Guzman et al., 2018; Huhtamo et al., 2014; Huhtamo et al., 2009).

Despite fundamental differences in their host ranges, flaviviruses share a common genomic organization. The genomic RNA is 10–11 kb in length and contains a long open reading frame flanked by 5’ and 3’ untranslated regions (UTRs) (Lindenbach, 2013). The open

reading frame encodes a polyprotein that is co- and post-translationally cleaved by the viral protease, host signal peptidases and host furin to produce three structural proteins, designated the capsid, premembrane/membrane (prM/M) and envelope (E) proteins, and seven nonstructural (NS) proteins in the gene order: 5′-C-prM(M)-E-NS1-NS2A-NS2B-NS3-NS4A-2K-NS4B-NS5–3′. Additional translational products are encoded by the genomes of select flaviviruses as a result of -1 ribosomal frameshifting (Firth et al., 2010; Melian et al., 2010).

The flavivirus E protein consists of three structural domains, designated as EDI, EDII and EDIII (Luca et al., 2012; Nybakken et al., 2006; Rey et al., 1995; Zhang et al., 2004). EDI mediates the conformation changes that occur in the endosome, EDII has important roles in dimerization and virus-mediated fusion and EDIII binds to host cell attachment factors and receptors during attachment and entry. The prM protein protects the E protein from undergoing an irreversible conformational change as the virion is secreted through acidified sorting compartments and is then cleaved into a soluble pr peptide and virion-associated M protein by *trans*-Golgi resident furin (Chen et al., 1996; Guirakhoo et al., 1992; Heinz et al., 1994; Rey et al., 1995; Stadler et al., 1997). The nonstructural proteins have multiple functions, but are primarily required for genome replication, immune evasion and viral assembly (Lindenbach, 2013). The NS5 protein functions as the viral RNA-dependent RNA polymerase and methyltransferase and inhibits host-mediated interferon signaling (Wang et al., 2018).

Chimeric viruses of WNV and BinJV have been generated and their *in vitro* host ranges assessed to identify the determinants that condition the vertebrate host range restriction of dISFs (Harrison et al., 2020; Hobson-Peters et al., 2019). One chimeric virus was created by substituting the prM-E genes of BinJV with the corresponding genes of WNV (Hobson-Peters et al., 2019). The reciprocal chimeric virus also created (Harrison et al., 2020). These studies provided evidence that the vertebrate host restriction of BinJV occurs at multiple steps in the virus replication cycle, including entry. Chimeric viruses have also been created by replacing the prM-E genes of BinJV with the corresponding genes of DENV1, DENV2, DENV4, JEV, YFV and ZIKV, with encouraging results produced in vaccine studies designed to determine whether these viruses protect vertebrate animals against MBFV disease (Hazlewood et al., 2020; Hobson-Peters et al., 2019; Vet et al., 2020; Yan et al., 2020). Studies have not been performed to identify the vertebrate host range restriction of any other dISFs. Here, we generated chimeras by replacing select regions of the ZIKV genome with the corresponding regions of dISFs, LPKV and LAMV, and characterized the *in vitro* host ranges of the resulting viruses to determine whether common or distinct processes mediate the vertebrate host range restriction of dISFs.

MATERIALS AND METHODS

Cell lines

Aedes albopictus (C6/36) and African Green Monkey kidney (Vero) cells were obtained from the American Type Culture Collection (Manassas, VA). C6/36 cells were cultured in Liebovitz L15 medium (Thermo Fisher Scientific, Carlsbad, CA) and Vero cells were cultured in Dulbecco's modified Eagle medium (Thermo Fisher Scientific). All media was

supplemented with 10% fetal bovine serum, 2 mM L-glutamine, 100 units/ml penicillin and 100 μg/ml streptomycin. C6/36 cells were cultured at 28°C and Vero cells were cultured at 37°C with 5% CO_2.

Viruses

LPKV (strain EVG 5–72) and ZIKV (PRVABC59) were obtained from the virus reference collections maintained at the University of Texas Medical Branch in Galveston, Texas. Viruses underwent no more than three additional passages in cell culture in our laboratories. LAMV (strain M0719) could not be acquired, but part of its genome (Genbank Accession No. NC_024806.1) was synthesized as a DNA fragment as described below.

Production of synthetic viral sequences

The genome of ZIKV was synthesized as three overlapping dsDNA fragments, designated as F1, F2 and F3 (Bio-Basic Inc., Markham, ON, Canada). F1 was 3992 bp in length and consisted of a modified *Orgyia pseudotsugata* multicapsid nucleopolyhedrosis virus immediate-early 2 promoter (OpIE2-CA) followed by ZIKV sequence (genomic position 1–3460) that spanned all of the 5’ UTR and structural genes and the first 971 nt. of the NS1 gene. OpIE2-CA has been used to generate Parramatta River and Palm Creek viruses in C6/36 cells transfected with cISF infectious cDNAs (Piyasena et al., 2017). F2 was 4659 bp in length, consisting of ZIKV sequence (genomic position 3413–8071) that encompassed the last 138 nt. of the NS1 gene, all of the NS2A to NS4B genes and the first 402 nt of the NS5 gene. F2 contains a 47 bp overlap with the 3’ end of F1. The fragment denoted as F3 is 3053 bp in length, spanning all of the ZIKV NS5 gene, except for the first 344 nt, and all of the 3’ UTR (genomic position 8016–10,807), followed by the hepatitis delta virus anti-genomic ribozyme sequence and simian virus 40 (SV40) polyadenylation signal (Varnavski et al., 2000). F3 contained a 57 bp overlap with the 3’ end of the F2. Fragments were blunt-end cloned into the Sma I restriction enzyme site of pUC19 (New England BioLabs, Ipswich MA) and the plasmids, designated as pUC19-F1, pUC19-F2 and pUC19-F3 according to the fragment they contained, were delivered to Iowa State University. A three-plasmid approach was used because full-length flavivirus cDNAs are usually toxic in bacteria (Aubry et al., 2015).

A dsDNA fragment, designated F1b, was also synthesized (Bio-Basic Inc.). F1b was 4001 bp in length, consisting of OpIE2-CA, followed by the 5’UTR and capsid gene sequences of ZIKV (genomic position 1–475), the prM-E gene sequences of LPKV (genomic position 405–2427) and most of the NS1 gene sequence of ZIKV (genome position 2490–3460). F1b had a 47 bp overlap with the 5’ end of F2. F1b was cloned into pUC19 and the resulting plasmid was designated as pUC19-F1b. Another dsDNA, designated F1c, was synthesized (Integrated DNA Technologies, Coralville IA). The 2084 bp fragment contained the complete prM-E gene sequences of LAMV (genomic position 442–2445) which were flanked at the 5’ and 3’ ends by the last 40 nt of the ZIKV capsid gene and first 40 nt of the ZIKV NS1 gene, respectively. F1c was provided as linear dsDNA.

Production of chimeras

Four viral chimeras were created by replacing the prM-E, E, EDIII and NS5 regions of ZIKV with those of LPKV, designated as cZIKV/LPKV-prME, cZIKV/LPKV-E, cZIKV/LPKV-EDIII and cZIKV/LPKV-NS5, respectively (Figure 1). An additional chimera was created by replacing the prM-E region of ZIKV with those of LAMV, designated as cZIKV/LAMV-prME. Initially, we attempted to create chimeras without using synthetically produced viral fragments, but this approach was less efficient, possibly because considerably more non-specific PCR products were produced, hindering chimera development.

To generate cZIKV/LPKV-prME, F1b, F2 and F3 were amplified from their respective plasmids, purified and joined together by Gibson assembly then transfected into C6/36 cells. The full-length ZIKV genome was assembled using the same approach, except that F1, F2 and F3 were used. Transfections were also performed using non-assembled DNA in the event that spontaneous recombination could occur in mosquito cells, as reported for vertebrate cells transfected with overlapping DNA fragments spanning entire MBFV genomes (Aubry et al., 2014). To generate cZIKV/LPKV-E, PCR was performed using pUC19-F1 as template, a forward primer specific to the distal 5’ end of the ZIKV NS1 gene and a reverse primer specific to the distal 3’ end of the ZIKV prM gene. This reaction amplified all of pUC19-F1, except for the E gene of ZIKV. A second PCR was performed using pUC19-F1b as template, along with a forward chimeric primer specific to the sequences at the distal 3’ and 5’ ends of the ZIKV prM and LPKV E genes, respectively and a reverse chimeric primer specific to the sequences at the distal 3’ and 5’ ends of the LPKV E and ZIKV NS1 genes, respectively. This reaction yielded an amplicon that contained the LPKV E gene flanked by the last 25 nt of the ZIKV capsid gene and first 25 nt of the ZIKV NS1 gene. The two amplicons were joined together by Gibson assembly and the resulting circular dsDNA was transformed into One Shot™ TOP10 chemically competent *E. coli* cells (ThermoFisher Scientific). A subset of colonies was selected and clones containing viral sequences with no mutations were identified. Plasmids were purified and used as template in a PCR designed to amplify all the chimeric viral sequence and none of the plasmid sequence. The product was used in a second Gibson assembly reaction together with F2 and F3 and the resulting circular dsDNA was transfected into C6/36 cells. A similar approach was used to generate cZIKV/LPKV-EDIII, except that the first PCR amplified all of pUC19-F1, except for the EDIII region of ZIKV, and the second PCR amplified the EDIII region of LPKV along with the appropriate 25 nt. flanking regions. Similar strategies were used to create cZIKV/LPKV-NS5 and cZIKV/LAMV-prME, although the LPKV NS5 gene was RT-PCR amplified using total RNA extracted from LPKV-infected C6/36 cells.

Gibson assembly

DNA fragments were assembled using Gibson Assembly Master Mix (New England BioLabs). Briefly, 350 ng of each of the required DNA fragments were mixed together, diluted in dH_20 and added to an equal volume of 2x Gibson Assembly Master Mix, to give a final reaction volume of 20 μl. Reactions were incubated at 50°C for 3 hr.

Transfections and virus recovery

Assembled DNAs were transfected into C6/36 cells using Lipofectamine™ 2000 Transfection Reagent (ThermoFisher Scientific). Transfections were also performed using non-assembled DNA. Each transfection was performed using 1,050 ng of DNA. Transfected C6/36 cells were incubated in six-well (9.6-cm^2) dishes for 7 days then a 50 μl aliquot of each supernatant was inoculated onto new monolayers of C6/36 in 25 cm^2 flasks. A second passage was then performed in C6/36 cells. Lysates and supernatants were harvested from the first and second cell culture passages at 5 days post-inoculation (p.i.) and assayed for virus.

Reverse transcription-polymerase chain reaction

Total RNA was extracted from cell monolayers and supernatants using Trizol Reagent (ThermoFisher Scientific) and the QIAamp viral RNA mini kit (Qiagen, Valencia, CA), respectively. Complementary DNAs were generated using Superscript III reverse transcriptase (ThermoFisher Scientific). PCRs were performed using high fidelity *Taq* polymerase (ThermoFisher Scientific). ZIKV, LPKV and LAMV-specific primers were designed using published sequences (Genbank Accession No. KX377337.1, KY290254.1.1 and NC_024806.1.1.1, respectively). All primer sequences used in this study are available upon request. RT-PCR products were examined by 1% agarose gel electrophoresis, purified using QIAquick spin columns (Qiagen) and sequenced using a 3730x1 DNA sequencer (Applied Biosystems, Foster City, CA).

Preparation of protein lysates

Cell monolayers, approaching confluency in 25 cm^2 flasks, were inoculated with ZIKV, LPKV or chimeric virus or they were mock inoculated, incubated for 1 hr. and rinsed three times with phosphate-buffered saline (PBS) to remove unbound virus particles. Fresh media was added and the cells were incubated for 4 days (Vero cells) or 5 days (C6/36 cells). Vero cells were incubated for less time than C6/36 cells because they developed cytopathic effect (CPE). Cells were scraped from the surface of the flask, clarified by centrifugation (10,000 g, 10 min, 4°C), washed twice with cold PBS, resuspended in lysing buffer [10 mM Tris–HCl pH 7.5, 150 mM NaC1, 5 mM EDTA, 1% sodium deoxycholate, 1% Triton X-100, 0.1% SDS and a cocktail of protease inhibitors (Sigma, St. Louis, MO)] and placed on ice for 15 min. Samples were microfuged at 4°C for 15 min and supernatants were collected and stored at −80°C.

Western blots

Protein samples were mixed with an equal volume of reducing sample buffer, heated (95°C for 5 min) and resolved on 8–16% Tris-glycine gels (ThermoFisher Scientific). Proteins were transferred to 0.45 μm nitrocellulose membranes (ThermoFisher Scientific) following published protocols (Towbin et al., 1979). Membranes were blocked for at least 1 h at 4°C in PBS, pH 7.2 with 5% (wt/vol) non-fat dried milk. Membranes were incubated with (i) 1/1000 rabbit anti-ZIKV prM polyclonal antibody (GeneTex Inc., Irvine, CA), (ii) 1/500 rabbit anti-ZIKV NS1 polyclonal antibody (GeneTex Inc.) or (iii) 1/1000 rabbit anti-β-actin polyclonal antibody (GeneTex) overnight at 4°C. Membranes were then washed and

incubated with 1/1000 horseradish peroxidase-conjugated goat anti-rabbit IgG antibody (ThermoFisher Scientific) for 1 h at room temperature. Specifically bound antibody was visualized using 3,3'-diaminobenzidine (0.05% in PBS with 0.018% H_2O_2).

Immunoflorescence assays

C6/36 and Vero cells were seeded on six-well (9.6-cm^2) dishes containing 18 mm diameter coverslips at a density of 1×10^5 cells/well and incubated at 28°C and 37°C, respectively until they reached confluency. Cells were inoculated with ZIKV, LPKV or chimeric virus or they were mock inoculated then incubated for 4 days (Vero cells) or 5 days (C6/36 cells). Cells were fixed either at −20°C for 3 min with 100% methanol or at room temperature for 10 min with 2% paraformaldehyde in PBS then washed three times with PBS. Fixed cells were permeabilized by incubation with 0.2% Triton X-100 in PBS for 5 min then washed three times with PBS. Cells were blocked for 10 min with 2% bovine serum albumin in PBS and incubated for 1 h with 1/500 rabbit anti-ZIKV capsid polyclonal antibody (Novus Biologicals, Littleton CO) or 1/500 rabbit anti-MBFV E protein 4G2 monoclonal antibody developed from DENV2 (Novus Biologicals). Cells were washed three times with PBS then incubated for an additional hour with 1/1000 Alexa 594-conjugated donkey anti-rabbit IgG (ThermoFisher Scientific). Immunostained cells were washed three times with PBS and mounted on slides with ProLong reagent with DAPI (4′,6-diamidino-2-phenylindole dihydrochloride) (ThermoFisher Scientific). Immunostained samples were examined with a Zeiss Axiovert 200 inverted microscope equipped with fluorescence optics. Images were prepared using Photoshop and Illustrator software (Adobe Systems).

RESULTS

Construction of chimeras of ZIKV and LPKV

Chimeras were created by replacing select regions of the ZIKV genome with the corresponding regions of the LPKV genome (Figure 1). Four genomic regions were selected: prM-E, E, EDIII and NS5. To create each chimera, overlapping cDNA fragments spanning the entire chimeric genome were joined together by Gibson assembly and transfected in C6/36 cells. Unassembled fragments were also transfected into C6/36 cells in the event that spontaneous recombination could occur in the cells. Recombinant ZIKV was also produced via the transfection of assembled and unassembled DNA fragments and used as a positive control.

Mosquito cells support ZIKV/LPKV-prME replication

The chimera created by substituting the prM-E genes of ZIKV with the corresponding genes of LPKV yielded infectious virus in C6/36 cells whereas the other chimeras did not (Figures 2 and 3, data not shown). The chimeric virus, designated ZIKV/LPKV-prME, was successfully generated by both the transfection of Gibson assembly products and unassembled DNA fragments that spanned the entire chimeric genome. Recombinant ZIKV was also successfully generated using both approaches. The results presented herein are for the viruses generated via the transfection of Gibson assembly products. Sanger sequencing revealed that there were no mutations in the prM-E genes and predicted C/prM and E/NS1 cleavage sites of the chimeric virus. Sanger sequencing also revealed that no mutations were

present in the LPKV sequences and predicted LPKV/ZIKV cleavage sites of the chimeras that failed to produce infectious virus.

ZIKV/LPKV-prME was maintained for at least six sequential passages in C6/36 cells, as determined in Western blots performed using anti-ZIKV NS1 polyclonal sera (Figure 2A). The intensity of the NS1 products decreased with each passage. Lysates harvested from the first two C6/36 cell passages were not included in this particular experiment. NS1 was also detected in ZIKV-inoculated C6/36 cells, but not LPKV-inoculated or uninfected C6/36 cells. Western blots performed using anti-ZIKV prM polyclonal sera did not detect a product in ZIKV/LPKV-prME-inoculated C6/36 cells (Figure 2B). Viral antigen was also not detected using anti-ZIKV prM polyclonal sera in LPKV-inoculated or uninfected C6/36 cells, but ZIKV-inoculated C6/36 cells were positive. Western blots performed using β-actin-specific polyclonal sera ensured that there was approximately equal loading in each lane (Figure 2C).

Immunofluorescence assays (IFAs) performed using anti-ZIKV capsid polyclonal sera and anti-MBFV E protein monoclonal antibody confirmed that ZIKV/LPKV-prME replicates in mosquito cells (Figure 3). Capsid antigen was detected in C6/36 cells inoculated with ZIKV/LPKV-prME and ZIKV. E antigen was also detected in cells inoculated with ZIKV. A weak fluorescent signal was observed in cells inoculated with ZIKV/LPKV-prME when the anti-MBFV E protein monoclonal antibody was used, suggesting weak cross-reactivity with LPKV. No signal was observed in the mock-inoculated C6/36 cell cultures. IFAs were also performed using LPKV-inoculated C6/36 cells, with no signal and a weak signal observed with the anti-ZIKV capsid polyclonal sera and anti-MBFV E protein monoclonal antibody, respectively (data not shown). These experiments were performed using ZIKV/LPKV-prME that had already undergone two sequential passages in C6/36 cells.

Vertebrate cells support ZIKV/LPKV-prME translation but not growth

To determine whether ZIKV/LPKV-prME is capable of vertebrate cell replication, the virus was sequentially passaged four times in Vero cells then the cells were assayed for viral antigen by Western blot and IFA (Figures 2, 4 and 5). Western blots performed using anti-ZIKV NS1 polyclonal sera revealed the presence of viral antigen in the first passage Vero cell cultures, but none of the subsequent passages (Figure 2A). NS1 was also detected in ZIKV-inoculated Vero cells but not LPKV-inoculated and uninfected Vero cells. When the anti-ZIKV prM polyclonal sera was used, antigen was only detected in ZIKV-inoculated Vero cells (Figure 2B). Western blots performed using β-actin-specific polyclonal sera ensured that there was approximately equal loading in each lane (Figure 2C). To determine whether translation of the chimeric virus genome had occurred in the first passage Vero cells or if we had detected only virus antigen present in the original inoculum, an additional experiment was performed where lysates were harvested at 1 hr. p.i. and tested by Western blot. Virus antigen was undetectable in these lysates (data not shown). These findings suggest that the virus antigen in the original inoculum was below the threshold of detection by Western blot analysis (data not shown).

IFAs confirmed the findings of the Western blot analysis. Viral antigen was detected by IFA in first, but not second, passage Vero cell cultures inoculated with ZIKV/LPKV-prME

(Figures 4 and 5). Viral antigen was undetectable by IFA in LPKV-inoculated Vero cells (data not shown). Vero cells inoculated with ZIKV/LPKV-prME appeared unhealthy despite their apparent inability to produce infectious virus (Figure 6). This observation was restricted to first passage Vero cell cultures, with all subsequent passages containing cells that were morphologically indistinguishable from uninfected control cells.

ZIKV/LAMV-prME replicates in mosquito but not vertebrate cells

A chimeric virus, designated as ZIKV/LAMV-prME, was produced by replacing the prM-E genes of the ZIKV genome with the corresponding regions of the LAMV genome. The chimeric virus was successfully generated by both the transfection of Gibson assembly products and unassembled DNA fragments that spanned the entire chimeric genome into C6/36 cells. Sanger sequencing revealed that the chimeric virus contained no mutations in its prM-E genes and predicted C/prM and E/NS1 cleavage sites. ZIKV/LAMV-prME could be maintained by sequential passaging in C6/36 cells but not Vero cells (Figures 3–5 and 7). Trace amounts of viral antigen were detected by IFA and Western blot in first passage Vero cell cultures inoculated with the chimeric virus (Figure 4 and 7). Additional IFAs were performed using Vero cells inoculated with increased amounts of virus and incubated for up to 7 days, yielding results consistent to those described above (data not shown). All Vero cell cultures inoculated with ZIKV/LPKV-prME were morphologically indistinguishable from uninfected control cultures (Figure 6). To bypass entry, ZIKV/LAMV-prME RNA was transfected into Vero cells, but infectious virus was still not recovered (data not shown).

Sequence comparison of the receptor-binding domains of ZIKV and select dISFs

The deduced amino acid sequences of the EDIIIs of LAMV, LPKV and ZIKV were aligned to provide insight into the apparent differential abilities of the major structural proteins of dISFs to permit vertebrate cell entry (Figure 8). BinJV was also included in the analysis. The alignment identified sites where residues were strictly conserved across all viruses, in addition to sites with conservative, semi-conservative and non-conservative replacements. Of the 93 sites, 29 were strictly conserved while 21, 12 and 31 contained conservative, semi-conservative and non-conservative replacements, respectively. Pairwise amino acid sequence alignments revealed that the EDIIs of the aforementioned dISFs are 51.1–54.4% identical. The EDIII of ZIKV is 48.9%, 46.7% and 46.7% identical to those of LAMV, LPKV and BinJV, respectively.

DISCUSSION

Chimeric viruses were created by replacing the prM-E genes of ZIKV with the corresponding regions of two dISFs, LPKV and LAMV. One other chimeric virus has been created by inserting genes of a dISF into the genomic backbone of a MBVF (Harrison et al., 2020). The chimeric virus, designated WNV_{KUN}/BinJV-prME, was generated by replacing the prM-E genes of WNV (subtype Kunjin virus) with those of BinJV, an *Aedes*-associated dISF, and it was capable of suboptimal entry into vertebrate cells. We detected modest amounts of viral antigen in vertebrate cells inoculated with ZIKV/LPKV-prME, but considerably more viral antigen was detected when ZIKV was used, suggesting that the major structural proteins of LPKV, like those of BinJV, also permit suboptimal vertebrate

cell entry. In contrast, trace amounts of virus antigen was detected in vertebrate cells inoculated with ZIKV/LAMV-prME, consistent with an almost complete block at entry. Our study provides evidence that the major structural proteins of dISFs possess differential abilities to facilitate entry into vertebrate cells.

Although viral antigen was detected in vertebrate cell cultures inoculated with chimeric ZIKVs containing the prM-E genes of LPKV and LAMV, infectious virus was not produced, as revealed by the absence of viral antigen in all subsequent cell culture passages. Viral antigen was also produced in first passage vertebrate cells inoculated with WNV_{KUN}/BinJV-prME, but supernatants were not assayed for infectious virus (Harrison et al., 2020). The data from our IFA and Western blotting experiments suggest that at least two blocks are responsible for the host range restriction of LPKV and LAMV, a partial to almost complete block at entry followed by another block after viral translation that completely abolishes infectious virus production. Stages in the viral lifecycle where the post-translational block likely occurs include virus assembly and egress.

Cytopathic effect was observed in first passage vertebrate cell cultures inoculated with ZIKV/LPKV-prME, despite the apparent lack of infectious virus production. One explanation for this finding is that the observed cellular morphological changes were caused by the chimeric virus passing through the plasma membrane. Viral translation requires the participation of many host proteins, disrupting normal cellular function, providing another explanation for the unhealthy appearance of the cells. Viral genome replication also involves the participation of many cellular proteins, although experiments were not performed to determine whether chimeric genome replication occurred. Another, potentially more likely, explanation is that apoptosis was induced by viral proteins. The C, prM, E and NS2A proteins and the NS2B-NS3 protease of various MBFVs possess pro-apoptotic activity in vertebrate cells (Bhuvanakantham et al., 2010; Catteau et al., 2003; Melian et al., 2013; Netsawang et al., 2010; Okamoto et al., 2017; Yang et al., 2009). Additionally, the C, prM, E, NS2B and NS4A proteins of ZIKV cause CPE in yeast cells (Li et al., 2017). CPE was not observed in vertebrate cell cultures inoculated with ZIKV/LAMV-prME, potentially because much less viral antigen was produced in these cells compared to those inoculated with ZIKV/LPKV-prME. Viability and apoptotic detection assays need to be performed to determine the molecular basis of the observed cellular morphological changes.

WNV_{KUN}/BinJV-prME replicated in mosquito cells, as did the two chimeric viruses produced in our study (Harrison et al., 2020). Replication of WNV_{KUN}/BinJV-prME in mosquito cells was suboptimal because it reached considerably lower titers than the parental viruses. One limitation of our study is the absence of time course experiments designed to compare the *in vitro* replication kinetics and yields of the chimeric and parental viruses. The findings from our sequential passaging experiments could indicate that chimeric virus replication was suboptimal because the intensity of the bands corresponding to NS1 of the chimeric viruses, but not ZIKV, decreased with each mosquito cell passage. However, quantitative measures are required to determine whether this is true. Viruses were not titrated after each passage. Initial cultures were inoculated at an MOI of 1.0, but subsequent passages were inoculated with equal volumes (20 μl), but not necessarily equal MOIs, of virus. Experiments designed to measure translation kinetics over time would have also

strengthen our study. Another limitation of our study is that vertebrate cells were not incubated at lower temperatures to determine whether their inability to support chimeric virus replication was due to a cell tropism restriction or a temperature-dependent restriction.

Different stages of the BinJV replication cycle are blocked in vertebrate cells (Harrison et al., 2020). Several blocks also impede the replication of cISFs in vertebrate cells (Junglen et al., 2017; Piyasena et al., 2019; Piyasena et al., 2017). Experiments performed with a Niénokoué virus replicon and a chimeric virus expressing the prM-E genes of Niénokoué virus in the genetic background of YFV revealed that vertebrate host range restriction of this cISF occurs due to blocks at attachment/entry, RNA replication and assembly/release (Junglen et al., 2017). Kamiti River virus could replicate in vertebrate cells when select interferon regulatory factors were knocked down suggesting that the vertebrate innate immune system is a major host restriction for cISF infection (Tree et al., 2016). Eilat virus, an insect-specific virus in the genus *Alphavirus*, cannot replicate in vertebrate cells because of blocks at viral entry and RNA replication (Nasar et al., 2015; Nasar et al., 2012). The nature of the insect host range restriction of vertebrate-specific flaviviruses has also been investigated (Charlier et al., 2004; Saiyasombat et al., 2014; Tumban et al., 2013).

A comparison of the deduced amino acid sequences of the EDIIIs of select dISFs, including LPKV and LAMV, provided no apparent explanation for the differential abilities of these viruses to enter vertebrate cells. Additionally, the chimera created by substituting the EDIII of ZIKV with the corresponding region of LPKV did not produce infectious virus. EDIII swaps have been successful when performed between other flaviviruses (Gallichotte et al., 2015; Gallichotte et al., 2019; McAuley et al., 2016; McElroy et al., 2006). Viruses were recovered when the EDIII of DENV4 was replaced with those of DENV2 and ZIKV (Gallichotte et al., 2015; Gallichotte et al., 2019). Viruses were also recovered when the EDIIIs of Bagaza virus, JEV, Koutango virus and St. Louis encephalitis virus were inserted into a genetic background of WNV (McAuley et al., 2016). EDIII substitutions between WNV and more distantly related flaviviruses, namely DENV2, Iguape virus, Powassan virus, YFV and ZIKV, were unsuccessful. The EDIIIs of the aforementioned recipient and donor viruses that yielded infectious virus have >65% amino acid identity, which is considerably higher than the 47% for ZIKV and LPKV. Interchanging the EDIIIs of highly divergent flaviviruses may cause improper folding of the E protein, rendering it non-functional.

Infectious virus was not produced from the chimeras created from E and NS5 gene substitutions. Replacement of the E gene of DENV4 with the corresponding region of tick-borne encephalitis virus also failed to produce virus (Pletnev et al., 1992). E gene exchanges between different DENV serotypes and between different WNV strains have been successful (Alsaleh et al., 2016; Siridechadilok et al., 2013). Virus was also produced after NS5 gene swaps were performed between different DENV serotypes and between different WNV strains (Setoh et al., 2015; Siridechadilok et al., 2013). However, chimeric DENV2 genomic RNA containing the NS5 gene of WNV failed to yield virus, unless co-transfected with wild-type DENV2 RNA (Dong et al., 2010). Swaps involving partial NS5 gene sequences have produced varying results (Khromykh et al., 1999; Teramoto et al., 2014). Complete gene swaps between heterologous flaviviruses are often unsuccessful, except those involving

prM-E gene sequences or closely related viral species. The divergence in sequence may result in functional incompatibilities between the replication machinery of the heterologous viruses or abolish certain protein-protein or protein-RNA interactions required for viral transport, assembly or immune evasion.

As noted above, the chimeras created from E, EDIII and NS5 substitutions did not yield infectious virus. It is unlikely that correct proteolytic processing of the polyproteins of the chimeras could not occur. Alignment of the deduced amino acid sequences of the ZIKV and LPKV polyproteins revealed that their predicted proteolytic cleavage sites are similar. Although the LPKV regions and junctions of all three non-viable chimeras were sequenced and revealed to contain no nucleotide errors, the constructs were not sequenced in their entirety and therefore, we cannot dismiss the possibility that there were lethal mutations outside the junctions that occurred during one of the PCR amplifications.

In summary, we provide evidence that the host range restriction of both LPKV and LAMV is imposed by blocks at least two stages of the virus replication cycle. Both viruses possess the capacity to enter vertebrate cells. LPKV entry is suboptimal. In contrast, LAMV entry appears to be almost fully suppressed, as indicated by the small number of viral antigen-positive cells and bands of weak intensity detected by IFA and Western blot, respectively. A second block occurs downstream of viral translation, completely ablating infectious LPKV and LAMV production. Future studies should be performed to determine whether similar blocks are responsible for the inability of *Culex*-associated dISFs to replicate in vertebrate cells.

FUNDING

This study was supported by a grant from the National Institutes of Health (R01AI114720).

REFERENCES

Alsaleh K, Khou C, Frenkiel MP, Lecollinet S, Vazquez A, de Arellano ER, Despres P, Pardigon N, 2016. The E glycoprotein plays an essential role in the high pathogenicity of European-Mediterranean IS98 strain of West Nile virus. Virology 492, 53–65. [PubMed: 26896935]

Aubry F, Nougairede A, de Fabritus L, Querat G, Gould EA, de Lamballerie X, 2014. Single-stranded positive-sense RNA viruses generated in days using infectious subgenomic amplicons. J Gen Virol 95, 2462–2467. [PubMed: 25053561]

Aubry F, Nougairede A, Gould EA, de Lamballerie X, 2015. Flavivirus reverse genetic systems, construction techniques and applications: a historical perspective. Antiviral Res 114, 67–85. [PubMed: 25512228]

Bhuvanakantham R, Cheong YK, Ng ML, 2010. West Nile virus capsid protein interaction with importin and HDM2 protein is regulated by protein kinase C-mediated phosphorylation. Microbes Infect 12, 615–625. [PubMed: 20417716]

Blitvich BJ, Firth AE, 2015. Insect-specific flaviviruses: a systematic review of their discovery, host range, mode of transmission, superinfection exclusion potential and genomic organization. Viruses 7, 1927–1959. [PubMed: 25866904]

Blitvich BJ, Firth AE, 2017. A Review of Flaviviruses that Have No Known Arthropod Vector. Viruses 9.

Bolling BG, Weaver SC, Tesh RB, Vasilakis N, 2015. Insect-Specific Virus Discovery: Significance for the Arbovirus Community. Viruses 7, 4911–4928. [PubMed: 26378568]

Catteau A, Kalinina O, Wagner MC, Deubel V, Courageot MP, Despres P, 2003. Dengue virus M protein contains a proapoptotic sequence referred to as ApoptoM. J Gen Virol 84, 2781–2793. [PubMed: 13679613]

Charlier N, Molenkamp R, Leyssen P, Paeshuyse J, Drosten C, Panning M, De Clercq E, Bredenbeek PJ, Neyts J, 2004. Exchanging the yellow fever virus envelope proteins with Modoc virus prM and E proteins results in a chimeric virus that is neuroinvasive in SCID mice. J Virol 78, 7418–7426. [PubMed: 15220415]

Chen Y, Maguire T, Marks RM, 1996. Demonstration of binding of dengue virus envelope protein to target cells. Journal of virology 70, 8765–8772. [PubMed: 8971005]

Colmant AMG, Hobson-Peters J, Bielefeldt-Ohmann H, van den Hurk AF, Hall-Mendelin S, Chow WK, Johansen CA, Fros J, Simmonds P, Watterson D, Cazier C, Etebari K, Asgari S, Schulz BL, Beebe N, Vet LJ, Piyasena TBH, Nguyen HD, Barnard RT, Hall RA, 2017. A New Clade of Insect-Specific Flaviviruses from Australian Anopheles Mosquitoes Displays Species-Specific Host Restriction. mSphere 2.

Crabtree MB, Sang RC, Stollar V, Dunster LM, Miller BR, 2003. Genetic and phenotypic characterization of the newly described insect flavivirus, Kamiti River virus. Arch Virol 148, 1095–1118. [PubMed: 12756617]

Dong H, Chang DC, Xie X, Toh YX, Chung KY, Zou G, Lescar J, Lim SP, Shi PY, 2010. Biochemical and genetic characterization of dengue virus methyltransferase. Virology 405, 568–578. [PubMed: 20655081]

Elrefaey AM, Abdelnabi R, Rosales Rosas AL, Wang L, Basu S, Delang L, 2020. Understanding the Mechanisms Underlying Host Restriction of Insect-Specific Viruses. Viruses 12.

Firth AE, Blitvich BJ, Wills NM, Miller CL, Atkins JF, 2010. Evidence for ribosomal frameshifting and a novel overlapping gene in the genomes of insect-specific flaviviruses. Virology 399, 153–166. [PubMed: 20097399]

Gallichotte EN, Widman DG, Yount BL, Wahala WM, Durbin A, Whitehead S, Sariol CA, Crowe JE Jr., de Silva AM, Baric RS, 2015. A new quaternary structure epitope on dengue virus serotype 2 is the target of durable type-specific neutralizing antibodies. mBio 6, e01461–01415. [PubMed: 26463165]

Gallichotte EN, Young EF, Baric TJ, Yount BL, Metz SW, Begley MC, de Silva AM, Baric RS, 2019. Role of Zika Virus Envelope Protein Domain III as a Target of Human Neutralizing Antibodies. mBio 10.

Guirakhoo F, Bolin RA, Roehrig JT, 1992. The Murray Valley encephalitis virus prM protein confers acid resistance to virus particles and alters the expression of epitopes within the R2 domain of E glycoprotein. Virology 191, 921–931. [PubMed: 1280384]

Guzman H, Contreras-Gutierrez MA, Travassos da Rosa APA, Nunes MRT, Cardoso JF, Popov VL, Young KI, Savit C, Wood TG, Widen SG, Watts DM, Hanley KA, Perera D, Fish D, Vasilakis N, Tesh RB, 2018. Characterization of Three New Insect-Specific Flaviviruses: Their Relationship to the Mosquito-Borne Flavivirus Pathogens. Am J Trop Med Hyg 98, 410–419. [PubMed: 29016330]

Harrison JJ, Hobson-Peters J, Colmant AMG, Koh J, Newton ND, Warrilow D, Bielefeldt-Ohmann H, Piyasena TBH, O'Brien CA, Vet LJ, Paramitha D, Potter JR, Davis SS, Johansen CA, Setoh YX, Khromykh AA, Hall RA, 2020. Antigenic Characterization of New Lineage II Insect-Specific Flaviviruses in Australian Mosquitoes and Identification of Host Restriction Factors. mSphere 5.

Hazlewood JE, Rawle DJ, Tang B, Yan K, Vet LJ, Nakayama E, Hobson-Peters J, Hall RA, Suhrbier A, 2020. A Zika Vaccine Generated Using the Chimeric Insect-Specific Binjari Virus Platform Protects against Fetal Brain Infection in Pregnant Mice. Vaccines (Basel) 8.

Heinz FX, Stiasny K, Puschner-Auer G, Holzmann H, Allison SL, Mandl CW, Kunz C, 1994. Structural changes and functional control of the tick-borne encephalitis virus glycoprotein E by the heterodimeric association with protein prM. Virology 198, 109–117. [PubMed: 8259646]

Hobson-Peters J, Harrison JJ, Watterson D, Hazlewood JE, Vet LJ, Newton ND, Warrilow D, Colmant AMG, Taylor C, Huang B, Piyasena TBH, Chow WK, Setoh YX, Tang B, Nakayama E, Yan K, Amarilla AA, Wheatley S, Moore PR, Finger M, Kurucz N, Modhiran N, Young PR, Khromykh AA, Bielefeldt-Ohmann H, Suhrbier A, Hall RA, 2019. A recombinant platform for flavivirus vaccines and diagnostics using chimeras of a new insect-specific virus. Sci Transl Med 11.

Hobson-Peters J, Yam AW, Lu JW, Setoh YX, May FJ, Kurucz N, Walsh S, Prow NA, Davis SS, Weir R, Melville L, Hunt N, Webb RI, Blitvich BJ, Whelan P, Hall RA, 2013. A new insect-specific flavivirus from northern Australia suppresses replication of West Nile virus and Murray Valley encephalitis virus in co-infected mosquito cells. PLoS One 8, e56534. [PubMed: 23460804]

Hoshino K, Isawa H, Tsuda Y, Yano K, Sasaki T, Yuda M, Takasaki T, Kobayashi M, Sawabe K, 2007. Genetic characterization of a new insect flavivirus isolated from Culex pipiens mosquito in Japan. Virology 359, 405–414. [PubMed: 17070886]

Huhtamo E, Cook S, Moureau G, Uzcategui NY, Sironen T, Kuivanen S, Putkuri N, Kurkela S, Harbach RE, Firth AE, Vapalahti O, Gould EA, de Lamballerie X, 2014. Novel flaviviruses from mosquitoes: mosquito-specific evolutionary lineages within the phylogenetic group of mosquito-borne flaviviruses. Virology 464–465, 320–329.

Huhtamo E, Putkuri N, Kurkela S, Manni T, Vaheri A, Vapalahti O, Uzcategui NY, 2009. Characterization of a novel flavivirus from mosquitoes in northern europe that is related to mosquito-borne flaviviruses of the tropics. J Virol 83, 9532–9540. [PubMed: 19570865]

Junglen S, Kopp A, Kurth A, Pauli G, Ellerbrok H, Leendertz FH, 2009. A new flavivirus and a new vector: characterization of a novel flavivirus isolated from uranotaenia mosquitoes from a tropical rain forest. J Virol 83, 4462–4468. [PubMed: 19224998]

Junglen S, Korries M, Grasse W, Wieseler J, Kopp A, Hermanns K, Leon-Juarez M, Drosten C, Kummerer BM, 2017. Host Range Restriction of Insect-Specific Flaviviruses Occurs at Several Levels of the Viral Life Cycle. mSphere 2.

Kenney JL, Solberg OD, Langevin SA, Brault AC, 2014. Characterization of a novel insect-specific flavivirus from Brazil: potential for inhibition of infection of arthropod cells with medically important flaviviruses. J Gen Virol 95, 2796–2808. [PubMed: 25146007]

Khromykh AA, Sedlak PL, Westaway EG, 1999. trans-Complementation analysis of the flavivirus Kunjin ns5 gene reveals an essential role for translation of its N-terminal half in RNA replication. J Virol 73, 9247–9255. [PubMed: 10516033]

Li G, Poulsen M, Fenyvuesvolgyi C, Yashiroda Y, Yoshida M, Simard JM, Gallo RC, Zhao RY, 2017. Characterization of cytopathic factors through genome-wide analysis of the Zika viral proteins in fission yeast. Proc Natl Acad Sci U S A 114, E376–E385. [PubMed: 28049830]

Lindenbach BD, Thiel H-J, Rice CM, 2013. Flaviviridae: the viruses and their replication, in: Knipe DM, Howley PM (Eds.), Fields Virology, 6th ed. Wolters Kluwer/Lippincott Williams & Wilkins Health, Philadelphia, PA, pp. 1101–1152.

Luca VC, AbiMansour J, Nelson CA, Fremont DH, 2012. Crystal structure of the Japanese encephalitis virus envelope protein. J Virol 86, 2337–2346. [PubMed: 22156523]

McAuley AJ, Torres M, Plante JA, Huang CY, Bente DA, Beasley DWC, 2016. Recovery of West Nile Virus Envelope Protein Domain III Chimeras with Altered Antigenicity and Mouse Virulence. J Virol 90, 4757–4770. [PubMed: 26912625]

McElroy KL, Tsetsarkin KA, Vanlandingham DL, Higgs S, 2006. Role of the yellow fever virus structural protein genes in viral dissemination from the Aedes aegypti mosquito midgut. J Gen Virol 87, 2993–3001. [PubMed: 16963758]

McLean BJ, Hobson-Peters J, Webb CE, Watterson D, Prow NA, Nguyen HD, Hall-Mendelin S, Warrilow D, Johansen CA, Jansen CC, van den Hurk AF, Beebe NW, Schnettler E, Barnard RT, Hall RA, 2015. A novel insect-specific flavivirus replicates only in Aedes-derived cells and persists at high prevalence in wild Aedes vigilax populations in Sydney, Australia. Virology 486, 272–283. [PubMed: 26519596]

Melian EB, Edmonds JH, Nagasaki TK, Hinzman E, Floden N, Khromykh AA, 2013. West Nile virus NS2A protein facilitates virus-induced apoptosis independently of interferon response. J Gen Virol 94, 308–313. [PubMed: 23114626]

Melian EB, Hinzman E, Nagasaki T, Firth AE, Wills NM, Nouwens AS, Blitvich BJ, Leung J, Funk A, Atkins JF, Hall R, Khromykh AA, 2010. NS1' of flaviviruses in the Japanese encephalitis virus serogroup is a product of ribosomal frameshifting and plays a role in viral neuroinvasiveness. J Virol 84, 1641–1647. [PubMed: 19906906]

Nasar F, Gorchakov RV, Tesh RB, Weaver SC, 2015. Eilat virus host range restriction is present at multiple levels of the virus life cycle. J Virol 89, 1404–1418. [PubMed: 25392227]

Nasar F, Palacios G, Gorchakov RV, Guzman H, Da Rosa AP, Savji N, Popov VL, Sherman MB, Lipkin WI, Tesh RB, Weaver SC, 2012. Eilat virus, a unique alphavirus with host range restricted to insects by RNA replication. Proc Natl Acad Sci U S A 109, 14622–14627. [PubMed: 22908261]

Netsawang J, Noisakran S, Puttikhunt C, Kasinrerk W, Wongwiwat W, Malasit P, Yenchitsomanus PT, Limjindaporn T, 2010. Nuclear localization of dengue virus capsid protein is required for DAXX interaction and apoptosis. Virus Res 147, 275–283. [PubMed: 19944121]

Nybakken GE, Nelson CA, Chen BR, Diamond MS, Fremont DH, 2006. Crystal structure of the West Nile virus envelope glycoprotein. J Virol 80, 11467–11474. [PubMed: 16987985]

Okamoto T, Suzuki T, Kusakabe S, Tokunaga M, Hirano J, Miyata Y, Matsuura Y, 2017. Regulation of Apoptosis during Flavivirus Infection. Viruses 9.

Pauvolid-Correa A, Solberg O, Couto-Lima D, Kenney J, Serra-Freire N, Brault A, Nogueira R, Langevin S, Komar N, 2015. Nhumirim virus, a novel flavivirus isolated from mosquitoes from the Pantanal, Brazil. Arch Virol 160, 21–27. [PubMed: 25252815]

Piyasena TBH, Newton ND, Hobson-Peters J, Vet LJ, Setoh YX, Bielefeldt-Ohmann H, Khromykh AA, Hall RA, 2019. Chimeric viruses of the insect-specific flavivirus Palm Creek with structural proteins of vertebrate-infecting flaviviruses identify barriers to replication of insect-specific flaviviruses in vertebrate cells. J Gen Virol.

Piyasena TBH, Setoh YX, Hobson-Peters J, Newton ND, Bielefeldt-Ohmann H, McLean BJ, Vet LJ, Khromykh AA, Hall RA, 2017. Infectious DNAs derived from insect-specific flavivirus genomes enable identification of pre- and post-entry host restrictions in vertebrate cells. Sci Rep 7, 2940. [PubMed: 28592864]

Pletnev AG, Bray M, Huggins J, Lai CJ, 1992. Construction and characterization of chimeric tick-borne encephalitis/dengue type 4 viruses. Proc Natl Acad Sci U S A 89, 10532–10536. [PubMed: 1438242]

Rey FA, Heinz FX, Mandl C, Kunz C, Harrison SC, 1995. The envelope glycoprotein from tick-borne encephalitis virus at 2 A resolution. Nature 375, 291–298. [PubMed: 7753193]

Roundy CM, Azar SR, Rossi SL, Weaver SC, Vasilakis N, 2017. Insect-Specific Viruses: A Historical Overview and Recent Developments. Adv Virus Res 98, 119–146. [PubMed: 28433051]

Saiyasombat R, Carrillo-Tripp J, Miller WA, Bredenbeek PJ, Blitvich BJ, 2014. Substitution of the premembrane and envelope protein genes of Modoc virus with the homologous sequences of West Nile virus generates a chimeric virus that replicates in vertebrate but not mosquito cells. Virol J 11, 150. [PubMed: 25151534]

Setoh YX, Prow NA, Rawle DJ, Tan CSE, Edmonds JH, Hall RA, Khromykh AA, 2015. Systematic analysis of viral genes responsible for differential virulence between American and Australian West Nile virus strains. J Gen Virol 96, 1297–1308. [PubMed: 25626681]

Siridechadilok B, Gomutsukhavadee M, Sawaengpol T, Sangiambut S, Puttikhunt C, Chin-inmanu K, Suriyaphol P, Malasit P, Screaton G, Mongkolsapaya J, 2013. A simplified positive-sense-RNA virus construction approach that enhances analysis throughput. J Virol 87, 12667–12674. [PubMed: 24049164]

Stadler K, Allison SL, Schalich J, Heinz FX, 1997. Proteolytic activation of tick-borne encephalitis virus by furin. J Virol 71, 8475–8481. [PubMed: 9343204]

Stollar V, Thomas VL, 1975. An agent in the Aedes aegypti cell line (Peleg) which causes fusion of Aedes albopictus cells. Virology 64, 367–377. [PubMed: 806166]

Teramoto T, Boonyasuppayakorn S, Handley M, Choi KH, Padmanabhan R, 2014. Substitution of NS5 N-terminal domain of dengue virus type 2 RNA with type 4 domain caused impaired replication and emergence of adaptive mutants with enhanced fitness. J Biol Chem 289, 22385–22400. [PubMed: 24904061]

Towbin H, Staehelin T, Gordon J, 1979. Electrophoretic transfer of proteins from polyacrylamide gels to nitrocellulose sheets: procedure and some applications. Proc Natl Acad Sci U S A 76, 4350–4354. [PubMed: 388439]

Tree MO, McKellar DR, Kieft KJ, Watson AM, Ryman KD, Conway MJ, 2016. Insect-specific flavivirus infection is restricted by innate immunity in the vertebrate host. Virology 497, 81–91. [PubMed: 27433779]

Tumban E, Maes NE, Schirtzinger EE, Young KI, Hanson CT, Whitehead SS, Hanley KA, 2013. Replacement of conserved or variable sequences of the mosquito-borne dengue virus 3' UTR with homologous sequences from Modoc virus does not change infectivity for mosquitoes. J Gen Virol 94, 783–788. [PubMed: 23255623]

Varnavski AN, Young PR, Khromykh AA, 2000. Stable high-level expression of heterologous genes in vitro and in vivo by noncytopathic DNA-based Kunjin virus replicon vectors. J Virol 74, 4394–4403. [PubMed: 10756054]

Vet LJ, Setoh YX, Amarilla AA, Habarugira G, Suen WW, Newton ND, Harrison JJ, Hobson-Peters J, Hall RA, Bielefeldt-Ohmann H, 2020. Protective Efficacy of a Chimeric Insect-Specific Flavivirus Vaccine against West Nile Virus. Vaccines (Basel) 8.

Wang B, Thurmond S, Hai R, Song J, 2018. Structure and function of Zika virus NS5 protein: perspectives for drug design. Cell Mol Life Sci 75, 1723–1736. [PubMed: 29423529]

Yan K, Vet LJ, Tang B, Hobson-Peters J, Rawle DJ, Le TT, Larcher T, Hall RA, Suhrbier A, 2020. A Yellow Fever Virus 17D Infection and Disease Mouse Model Used to Evaluate a Chimeric Binjari-Yellow Fever Virus Vaccine. Vaccines (Basel) 8.

Yang TC, Shiu SL, Chuang PH, Lin YJ, Wan L, Lan YC, Lin CW, 2009. Japanese encephalitis virus NS2B-NS3 protease induces caspase 3 activation and mitochondria-mediated apoptosis in human medulloblastoma cells. Virus Res 143, 77–85. [PubMed: 19463724]

Zhang Y, Zhang W, Ogata S, Clements D, Strauss JH, Baker TS, Kuhn RJ, Rossmann MG, 2004. Conformational changes of the flavivirus E glycoprotein. Structure 12, 1607–1618. [PubMed: 15341726]

Research Highlights

- Several chimeras of Zika virus and select insect-specific flaviviruses were created
- Chimeric ZIKVs with prM-E genes of ISFs replicated in mosquito cells
- Chimeric ZIKVs with prM-E genes of ISFs could not replicate in vertebrate cells
- Entry and post-translational restrictions prevented replication in vertebrate cells

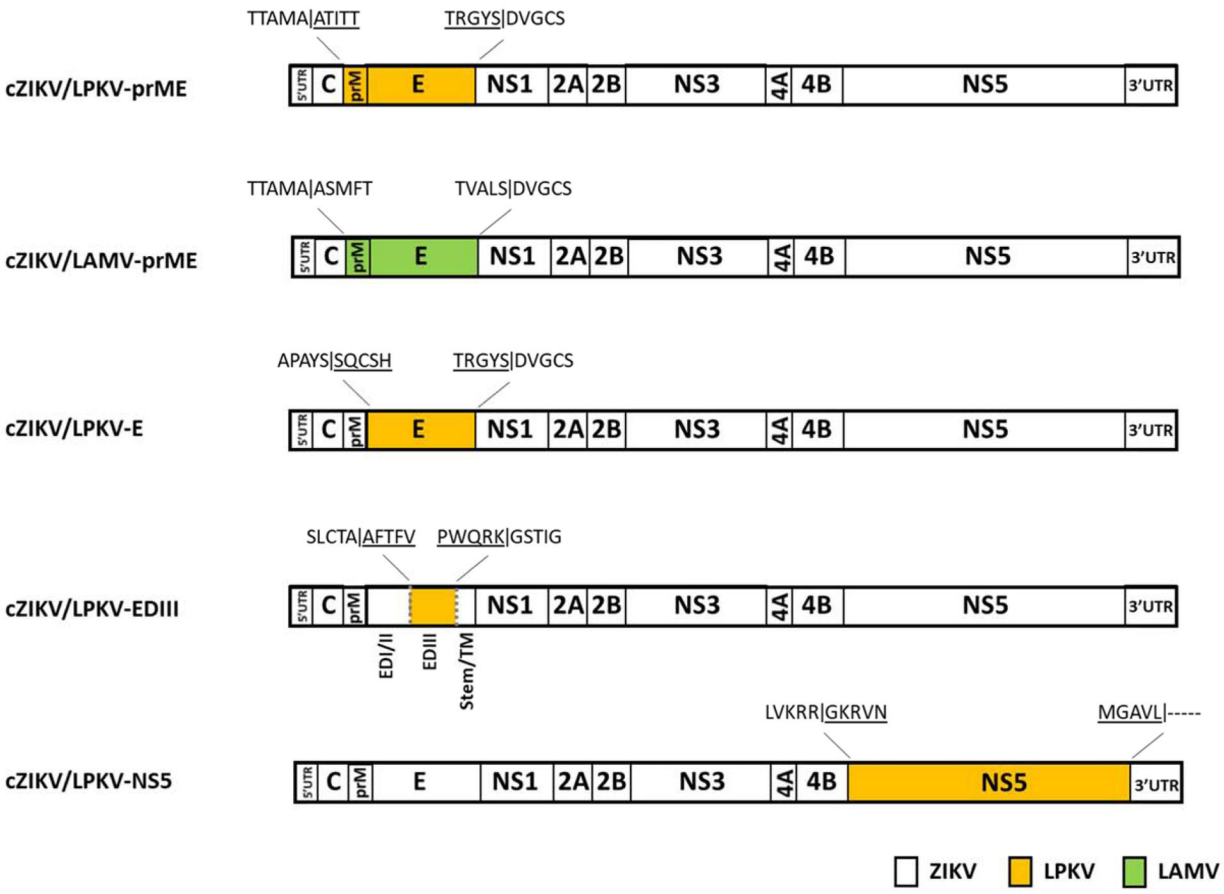

FIGURE 1.

A schematic of the viral chimeras produced in this study. Four chimeras were generated by replacing the prM-E, E, EDIII and NS5 regions of ZIKV with those of LPKV (denoted as cZIKV/LPKV-prME, cZIKV/LPKV-E, cZIKV/LPKV-EDIII and cZIKV/LPKVNS5) and an additional chimera was generated by replacing the prM-E region of ZIKV with those of LAMV (denoted as cZIKV/LAMV-prME). Each chimera name begins with a lowercase c to differentiate between viral chimeras and infectious chimeric viruses. In the schematic representing cZIKV/LPKV-EDIII, the location of EDIII within the E region is denoted, along with EDI, EDII, the stem region and transmembrane (TM) domain. The short hinge region that immediately precedes EDIII is not shown. Resulting amino acid chimeric sequences are denoted, with protease cleavage sites indicated by vertical lines. Sequences from the heterologous viruses (LPKV and LAMV) are underlined.

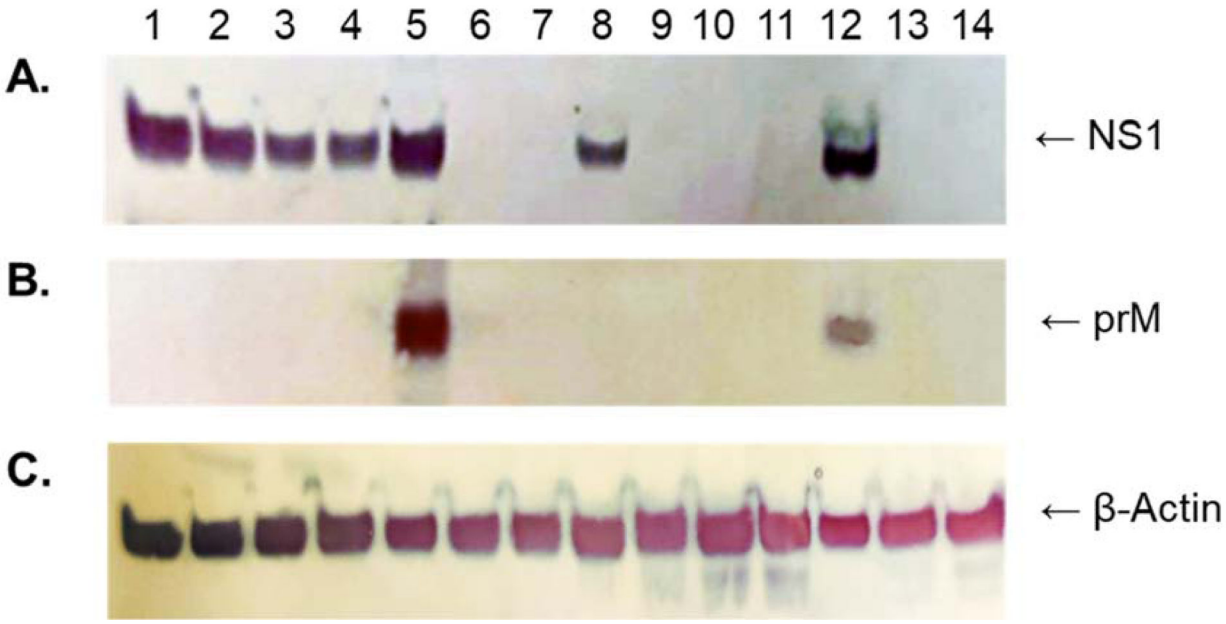

FIGURE 2.

Western blot analysis of mosquito and vertebrate cells inoculated with ZIKV/LPKV-prME. The chimeric virus was passaged twice in C6/36 cells then sequentially passaged four more times in C6/36 cells (lanes 1–4, passage 3–6 respectively) or four times in Vero cells (lanes 8–11, Vero cell passage 1–4 respectively). C6/36 and Vero cells inoculated with ZIKV (lanes 5 and 12, respectively) and LPKV (lanes 6 and 13, respectively) were also included. Uninfected C6/36 and Vero cells were used as negative controls (lanes 7 and 14, respectively). Lysates were prepared at 4 or 5 days post-inoculation (Vero and C6/36 cells, respectively). Equal amounts of protein were resolved on 8–16% Tris-glycine gels and analyzed by Western blot using (A) anti-ZIKV NS1 polyclonal antibody, (B) anti-ZIKV prM polyclonal antibody or (C) anti-β-actin polyclonal antibody. The arrows show the expected migration positions of ZIKV prM and NS1 (molecular weights: 19 and 48 KDa, respectively) and cellular β-actin (molecular weight: 42 KDa).

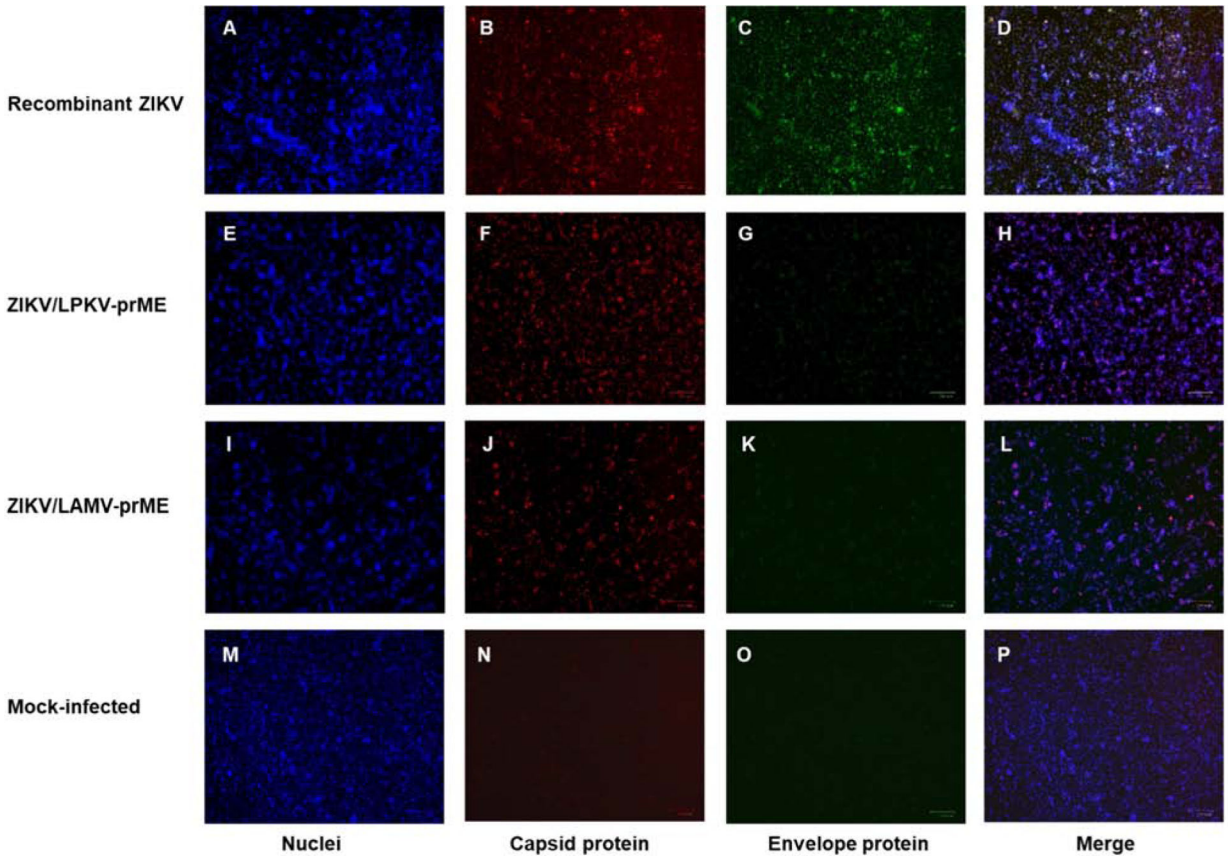

FIGURE 3.

Immunofluorescence analysis of mosquito cells inoculated with ZIKV/LPKV-prME and ZIKV/LAMV-prME. Subconfluent monolayers of C6/36 cells in six-well culture dishes were inoculated with recombinant ZIKV, ZIKV/LPKV-prME or ZIKV/LAMV-prME at a multiplicity of infection (MOI) of 1.0 or they were inoculated with media only (rows 1–4, respectively). Both chimeric viruses had undergone two passages in C6/36 cells prior to the experiment. At 5 days post-inoculation, cells were fixed with methanol and immunostained with anti-ZIKV capsid polyclonal antibody (column 2) or pan-flavivirus E protein monoclonal antibody (column 3), followed by Alexa 594-conjugated donkey anti-rabbit IgG. DAPI was used to visualize the nucleic (column 1). Merged images are also shown (column 4).

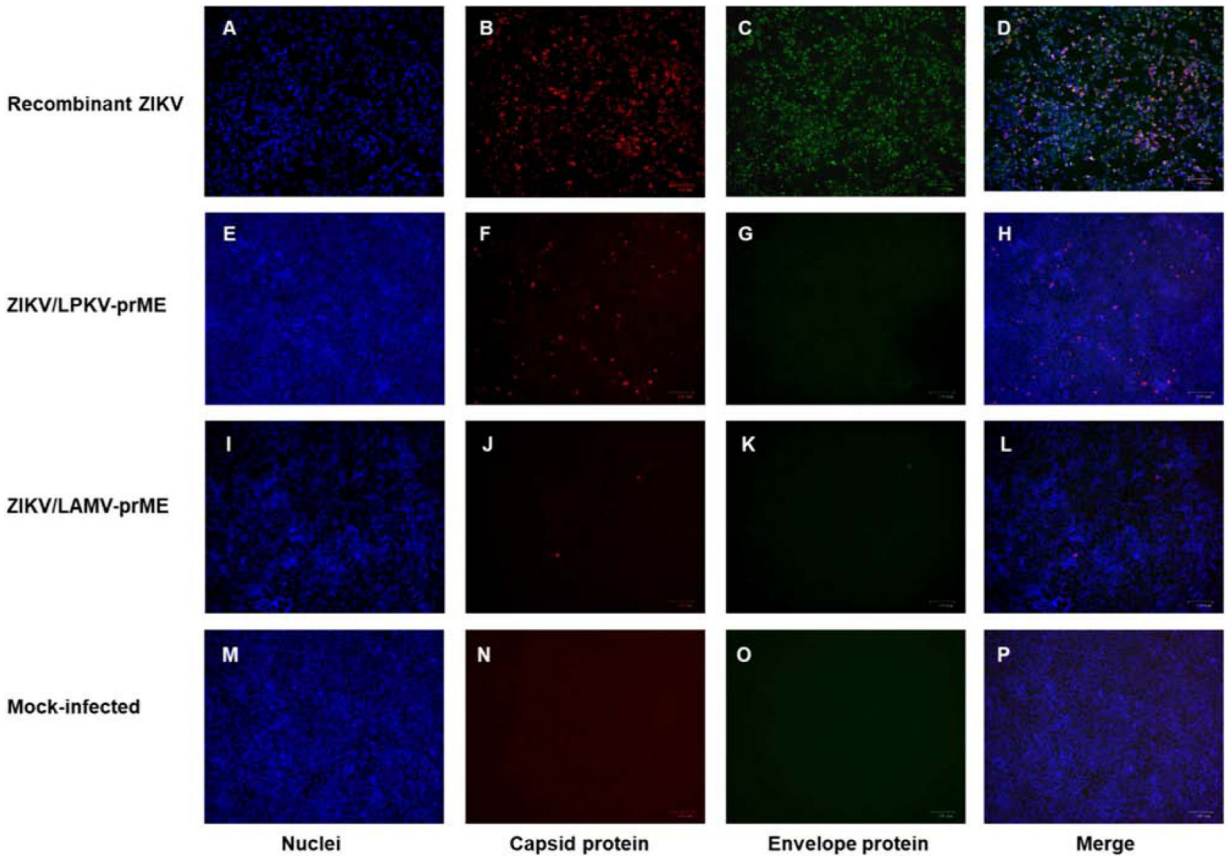

FIGURE 4.

Monitoring first passage Vero cell cultures for ZIKV/LPKV-prME and ZIKV/LAMV-prME antigens by immunofluorescence assay. Subconfluent monolayers of Vero cells in six-well culture dishes were inoculated with recombinant ZIKV, ZIKV/LPKV-prME, ZIKV/LAMV-prME at an MOI of 1.0 or they were inoculated with media only (rows 1–4, respectively). Viruses had undergone two passages in C6/36 cells prior to the experiment. At 4 days post-inoculation, cells were fixed with methanol and immunostained with anti-ZIKV capsid polyclonal antibody (column 2) or pan-flavivirus E protein monoclonal antibody (column 3), followed by Alexa 594-conjugated donkey anti-rabbit IgG. DAPI was used to visualize the nucleic (column 1). Merged images are also shown (column 4).

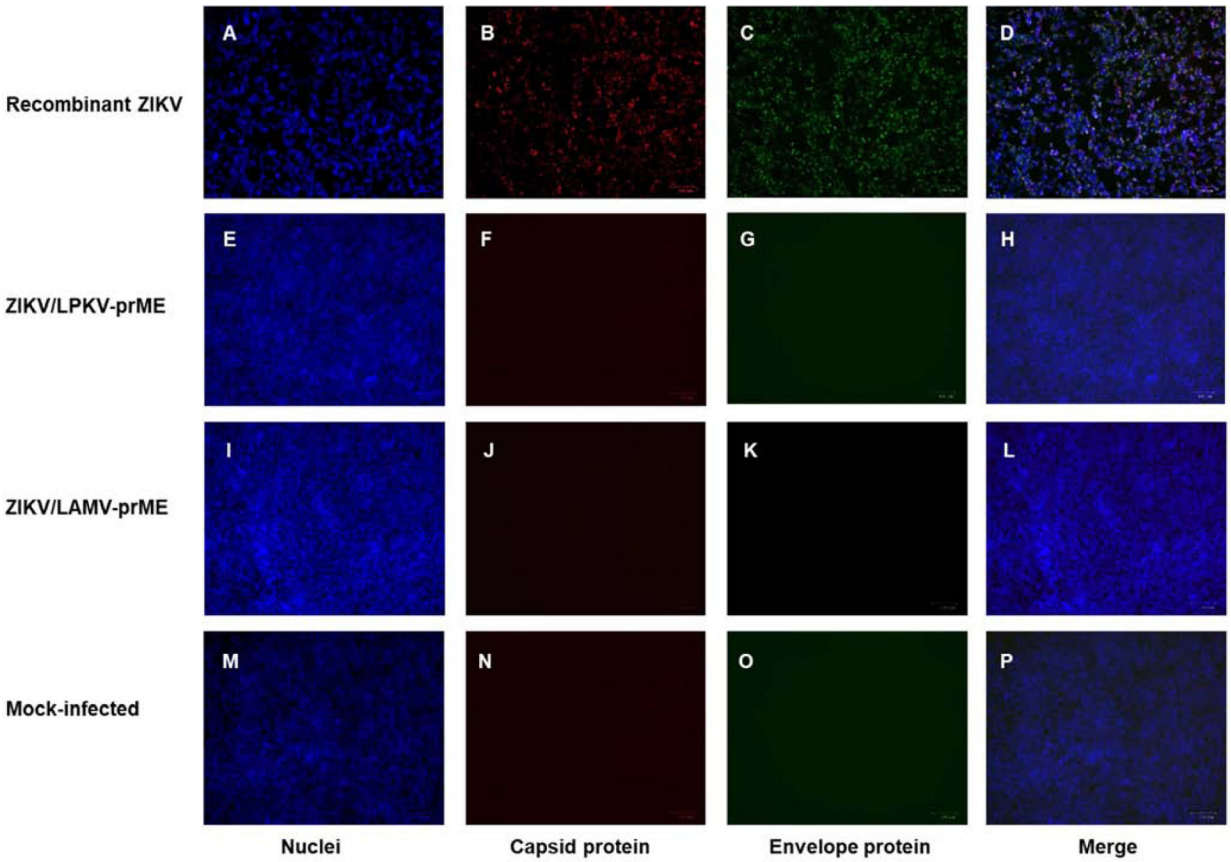

FIGURE 5.

Monitoring second passage Vero cell cultures for ZIKV/LPKV-prME and ZIKV/LAMV-prME antigens by immunofluorescence assay. Subconfluent monolayers of Vero cells in six-well culture dishes were inoculated with recombinant ZIKV, ZIKV/LPKV-prME, ZIKV/LAMV-prME or media only (rows 1–4, respectively). Viruses had undergone two passages in C6/36 cells followed by one passage in Vero cells prior to the experiment. At 4 days post-inoculation, cells were fixed with methanol and immunostained with anti-ZIKV capsid polyclonal antibody (column 2) or pan-flavivirus E protein monoclonal antibody (column 3), followed by Alexa 594-conjugated donkey anti-rabbit IgG. DAPI was used to visualize the nucleic (column 1). Merged images are also shown (column 4).

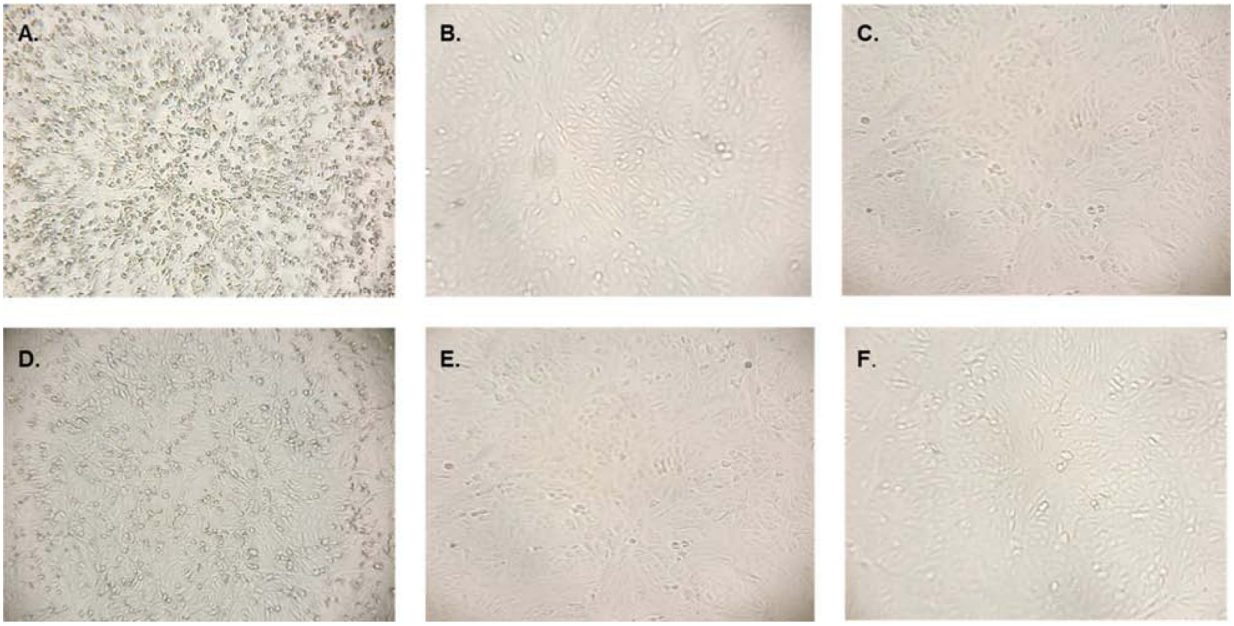

FIGURE 6.

Morphology of vertebrate cells inoculated with the chimeric viruses. Subconfluent monolayers of Vero cells in six-well dishes were inoculated with (A) recombinant ZIKV, (B) wild-type LPKV, (C) media only as a negative control, (D) ZIKV/LPKV-prME previously passed twice in C6/36 cells (E) ZIKV/LPKV-prME previously passed twice in C6/36 cells followed by once in Vero cells and (F) ZIKV/LAMV-prME previously been passed twice in C6/36 cells. Images were taken at 4 days post-inoculation (ZIKV) or 7 days post-inoculation (all other cultures).

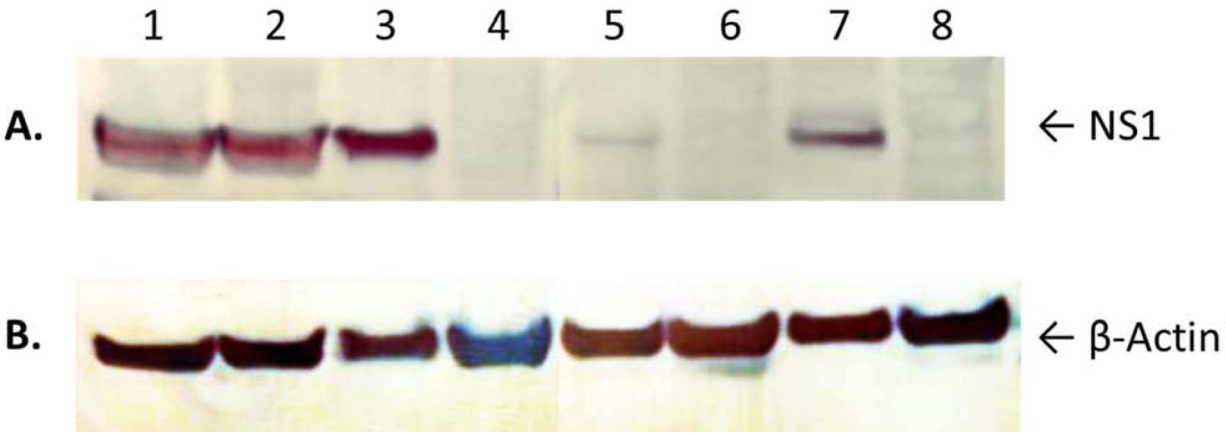

FIGURE 7.

Western blot analysis of lysates harvested from mosquito and vertebrate cells inoculated with ZIKV/LAMV-prME. The chimeric virus was passaged twice in C6/36 cells then sequentially passaged two more times in C6/36 cells (lanes 1–2, passage 3–4 respectively) or two times in Vero cells (lanes 5–6, Vero cell passage 1–2 respectively). C6/36 and Vero cells inoculated with ZIKV (lanes 3 and 7, respectively) were also included. Uninfected C6/36 and Vero cells were used as negative controls (lanes 4 and 8, respectively). Lysates were prepared at 4 or 5 days post-inoculation (Vero and C6/36 cells, respectively). Equal amounts of protein were resolved on 8–16% Tris-glycine gels and analyzed by Western blot using (A) anti-ZIKV NS1 polyclonal antibody or (B) anti-β-actin polyclonal antibody. The arrows show the expected migration positions of ZIKV NS1 and cellular β-actin (molecular weights: 48 KDa and 42 KDa, respectively).

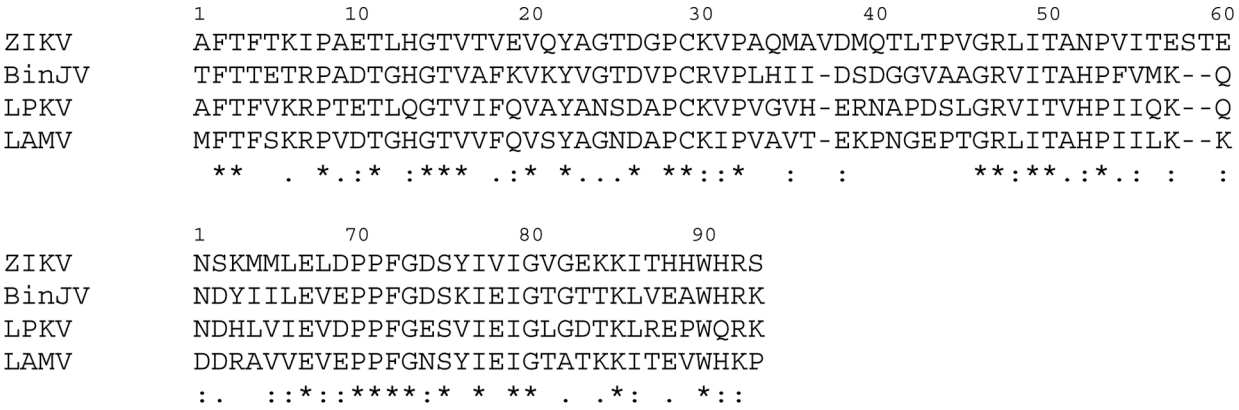

FIGURE 8.

Alignment of the deduced amino acid sequences of the EDIII domains of select flaviviruses. The key beneath the alignment denotes sites where residues are strictly conserved across all sequences (*), sites with conservative replacements (:), sites with semi-conservative replacements (.) and sites with non-conservative replacements ( ). The alignment was performed using Clustal Omega (https://www.ebi.ac.uk/Tools/msa/clustalo/). BinJV, Binjari virus; LAMV, Lammi virus; LPKV, Long Pine Key virus; ZIKV, Zika virus.